Synergistic effects of TiO$_2$ photocatalysis in combination with Fenton-like reactions on oxidation of organic compounds at circumneutral pH

Hyung-Eun Kim[a], Jaesang Lee[b], Hongshin Lee[a], Changha Lee[a,*]

[a] School of Urban and Environmental Engineering, Ulsan National Institute of Science and Technology (UNIST), 100 Banyeon-ri, Eonyang-eup, Ulju-gun, Ulsan 698-805, Republic of Korea
[b] Water Research Center, Korea Institute of Science and Technology (KIST), Seoul 136-791, Republic of Korea

ABSTRACT

The integration of two different AOPs often offers synergistic reaction routes for the production of •OH. In this study, synergistic production of •OH was observed in the combined system of TiO$_2$ photocatalysis and the Fenton-like reaction, causing a drastic enhancement in the oxidation of organic compounds at circumneutral pH values. The photolytic experiments using organic substrates (i.e., phenol, benzoic acid, and methanol) and valence band hole and •OH scavengers (i.e., formate and *tert*-butyl alcohol) show that the synergistic effects result from dual roles of iron as an electron acceptor to facilitate charge separation in TiO$_2$ photocatalyst and as a Fenton reagent to catalyze conversion of H$_2$O$_2$ into •OH. A noteworthy observation is that the adsorption of iron onto the photoexcited TiO$_2$ surface possibly modifies electron transfer properties of iron toward H$_2$O$_2$ at neutral pH to convert the resultant reactive oxidant from Fe(IV) into a stronger form, likely •OH.

© 2011 Elsevier B.V. All rights reserved.

1. Introduction

Advanced oxidation processes (AOPs) have emerged as promising alternative strategies to traditional options of adsorption, bioremediation, and coagulation/flocculation due to their capability of rapid degradation of a wide range of recalcitrant pollutants in the aquatic environment. Such effective remediation of aquatic hazardous substances is attributed to in situ generation of hydroxyl radical (•OH) as a primary transient oxidant. •OH exhibits nonselective reactivity toward diverse organic compounds thus initiating diffusion-limited oxidation reactions [1]. As a result, many technical efforts have been put forth to improve the efficiency of AOPs toward oxidative decontamination by enhancing the production rate of •OH, which includes the introduction of chemical additives (e.g., H$_2$O$_2$, S$_2$O$_8^{2-}$, and SiW$_{12}$O$_{40}^{4-}$) [2–4], utilization of external energy (e.g., UV, ultrasound, microwave) [5–7], surface modifications of reagents and catalysts (e.g., nanoscale metallization, coupled semiconductor systems) [8,9], and the integration of two or more AOPs [10–12].

It is recognized that in certain cases, the combination of AOPs can lead to drastic enhancement in •OH production (beyond the sum of the yields of •OH from the individual AOP) by offering synergistic reaction routes to key mechanisms involving •OH formation. For instance, when TiO$_2$ photocatalysis is combined with ozonation, the efficacies of both the systems for the production of •OH are enhanced [10]. Ozone inhibits the hole–electron recombination by scavenging conduction band (CB) electrons of photo-excited TiO$_2$ to increase the lifetime of valance band hole and subsequently generates more •OH. At the same time, the resultant ozonide radical anions accelerate the chain reactions of ozone decomposition into •OH.

Similarly, the combination of TiO$_2$ photocatalysis (the UV/TiO$_2$ system) with the Fenton system can lead to drastic enhancement in the production of •OH. Several previous studies have reported the enhanced oxidation of contaminants by the UV/TiO$_2$ system in the presence of ferric ion (Fe[III]) [13], the simultaneous addition of Fe(III) and H$_2$O$_2$ [11], and iron-doped TiO$_2$ [14,15]. However, it has not been clearly addressed whether the integration of the UV/TiO$_2$ and Fe(III)/H$_2$O$_2$ systems exhibits synergistic results with respect to the degradation of the contaminant. Moreover, little data is available on the role of iron in the UV/TiO$_2$ system under neutral pH conditions, where the Fe(III)/H$_2$O$_2$ (or UV/Fe(III)/H$_2$O$_2$) system alone is not effective for reactive oxidant production and relevant pollutant oxidation due to the low aqueous iron solubility and H$_2$O$_2$ decomposition via a nonradical mechanism (not leading to •OH generation) [2,16].

This study shows that the synergistic combination of TiO$_2$ photocatalysis and Fenton-like reaction (Fe(III)/H$_2$O$_2$) causes drastic

kinetic enhancement in pollutant oxidation under circumneutral pH conditions that are detrimental to Fenton oxidation. The feasible mechanism for such synergism is suggested based on the kinetics experiments using organic substrates, which have different reactivity toward the oxidizing species including $^\bullet OH$, ferryl ion (Fe[IV]), and valence band (VB) hole.

2. Experimental

2.1. Reagents

All chemicals were of reagent grade and were used as received except for 2,4-dinitrophenyl hydrazine (DNPH). DNPH was recrystalized from acetonitrile three times prior to use. All chemicals were obtained from Sigma–Aldrich except for acetonitrile (J.T. Baker) and TiO_2 powder (Degussa). Degussa P25 consisting of 80% anatase and 20% rutile was used as a titanium dioxide (TiO_2) photocatalyst. All the stock and buffer solutions were prepared in $18\,M\Omega$ Milli-Q water from a Millipore system. The Fe(III) stock solution (50 mM) was prepared by dissolving $Fe(ClO_4)_3\,6H_2O$ in 0.1 N $HClO_4$ solution. Stock solutions of H_2O_2 (10.2 M), phenol (10 mM), and benzoic acid (10 mM) were prepared prior to experiments.

2.2. Experimental apparatus and procedure

All the experiments were performed in a batch system using a 100 mL Pyrex flask open to the atmosphere at room temperature ($22 \pm 2\,^\circ C$). Photochemical experiments were performed in a dark chamber equipped with 4 W Black Light Blue (BLB) lamps (Philips. Co; $\lambda_{max} = 365$ nm), a sampling port, a stirrer, and a cooling fan. The incident photon flow (light intensity) of the setup for the photochemical experiments was measured to be 5.3×10^{-7} Einstein $L^{-1}\,s^{-1}$ by ferrioxalate actinometry [17].

Reaction solutions were unbuffered except for pH 9 (10 mM borate buffer), and the pH variation was monitored after the reaction. The initial pH of solutions was adjusted with 1 N NaOH and 1 N $HClO_4$ after adding catalysts and organic compounds. The reaction was initiated by adding H_2O_2 (simultaneously starting the UV irradiation for photochemical experiments). Samples were withdrawn at predetermined time intervals, and filtered immediately using a $0.45\,\mu m$ nylon syringe filter and a glass syringe. For the experiments with phenol and benzoic acid, $50\,\mu L$ of methanol was added to 1 mL of filtered solutions to quench the reaction. All the experiments were carried out at least in duplicate and average values and the standard deviations are presented.

2.3. Analytical methods

Phenol and benzoic acid were analyzed by high performance liquid chromatography (HPLC, UltiMate^{TM} 3000, Dionex Co.) with UV absorbance detection at 270 and 254 nm, respectively. Formaldehyde (HCHO), the primary oxidation product of methanol, was analyzed by HPLC with UV absorbance detection at 350 nm after DNPH derivatization [18]. Separation was performed on a Acclaim 120 C18 column (250 mm × 4.6 mm, $5\,\mu m$), using water with 1 mM nitric acid and acetonitrile as the eluent in a ratio of 50: 50, at a flow rate of $1.0\,mL\,min^{-1}$. The concentration of Fe(II) and H_2O_2 were measured spectrophotometrically by the 1,10-phenanthroline and titanium sulfate methods, respectively, using a S-3100 UV/vis spectrophotometer (Scinco Co.) [19,20]. The surface morphology and the element distribution of TiO_2 before and after the photochemical experiments with Fe(III) and H_2O_2 were determined using a Quanta 200 (Fei Co.) scanning electron microscope coupled with a energy dispersive X-ray spectrometer (SEM/EDX) at an accelerating voltage of 10 kV.
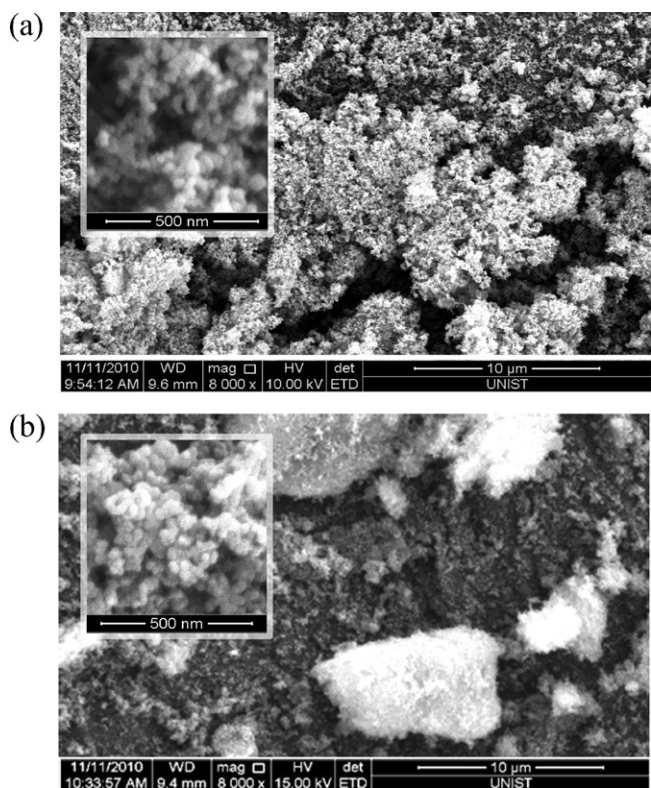

Fig. 1. SEM images of Degussa P25 TiO_2 (a) before and (b) after the reaction in UV/TiO_2/Fe(III)/H_2O_2 system ([Fe(III)] = 0.25 mM; TiO_2 = 1 g/L; [H_2O_2] = 10 mM; reaction time = 30 min).

3. Results and discussion

3.1. Surface characterization of TiO_2 particulates

SEM images show that TiO_2 particles undergo further aggregation during the photocatalytic reactions in the UV/TiO_2/Fe(III)/H_2O_2 system (Fig. 1a and b). Amorphous precipitates of Fe(III)-oxyhydroxides adsorbed on the TiO_2 surface, possibly neutralizes the surface charge, resulting in additional clustering of the TiO_2 particles. The EDX spectra of TiO_2 particles obtained after UV irradiation in the presence of Fe(III) and H_2O_2 verified the uniform presence of iron species on TiO_2 surface (Fig. 2). EDX analysis further quantified the surface iron content as 2.2 wt% (the average value of the two measurements in Fig. 2, excluding the platinum content from the sputter coating), which was slightly higher than the iron loading estimated from the applied concentration of Fe(III) (0.25 mmol iron/1 g TiO_2 = 1.4 wt%).

3.2. Enhanced degradation of organic compounds in the combined UV/TiO_2/Fe(III)/H_2O_2 system

Fig. 3a shows the effect of Fe(III) on the kinetics of degradation of phenol and benzoic acid by the UV/TiO_2/H_2O_2 system at neutral pH. Phenol and benzoic acid were degraded at almost similar rates. Dark adsorption and UV direct photolysis caused no significant loss of phenol and benzoic acid (data not shown). Addition of ferric ion significantly enhanced the oxidation of phenol and benzoic acid: the degradation followed pseudo first-order kinetics and the rate constants in the presence of Fe(III) (3.6–3.7×10^{-2} min^{-1}) were approximately 3.5–4 times faster than those in the absence of Fe(III) (0.95–1.0×10^{-2} min^{-1}). Fig. 3b shows the kinetics of H_2O_2 decomposition during the photocatalyzed degradation of phenol and benzoic acid. The presence of Fe(III) significantly accelerated

| Element	Wt%	At%
C	01.95	05.64
O	23.18	50.34
Pt	18.48	03.29
Ti	54.75	39.71
Fe	01.64	01.02

Element	Wt%	At%
C	02.85	07.85
O	26.60	55.05
Pt	22.00	03.73
Ti	46.73	32.29
Fe	01.82	01.08
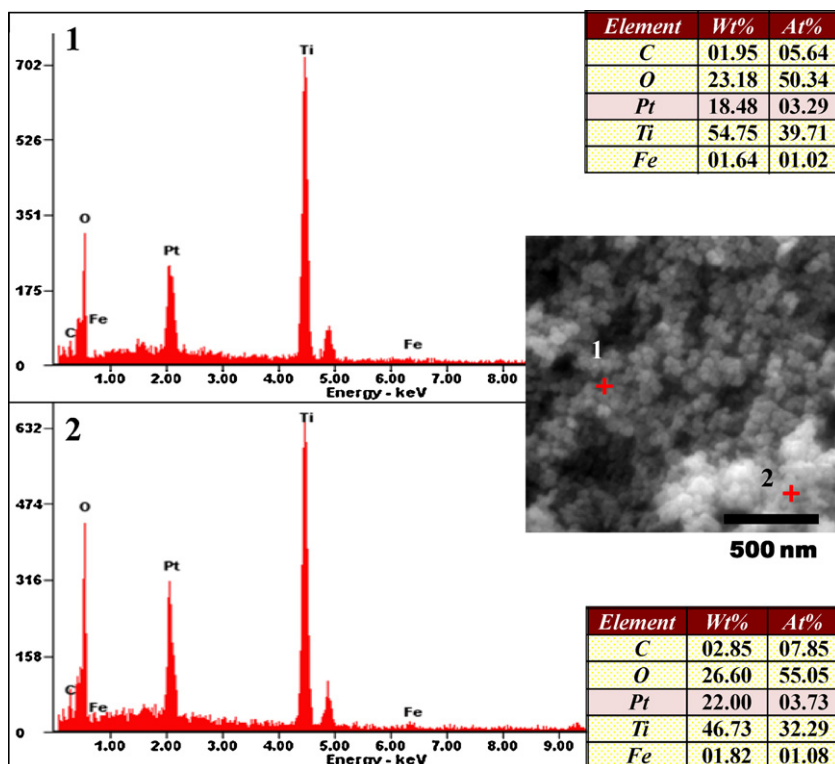
Fig. 2. EDX spectra of TiO_2 after the reaction in $UV/TiO_2/Fe(III)/H_2O_2$ system ([Fe(III)] = 0.25 mM; TiO_2 = 1 g/L; [H_2O_2] = 10 mM; reaction time = 30 min).
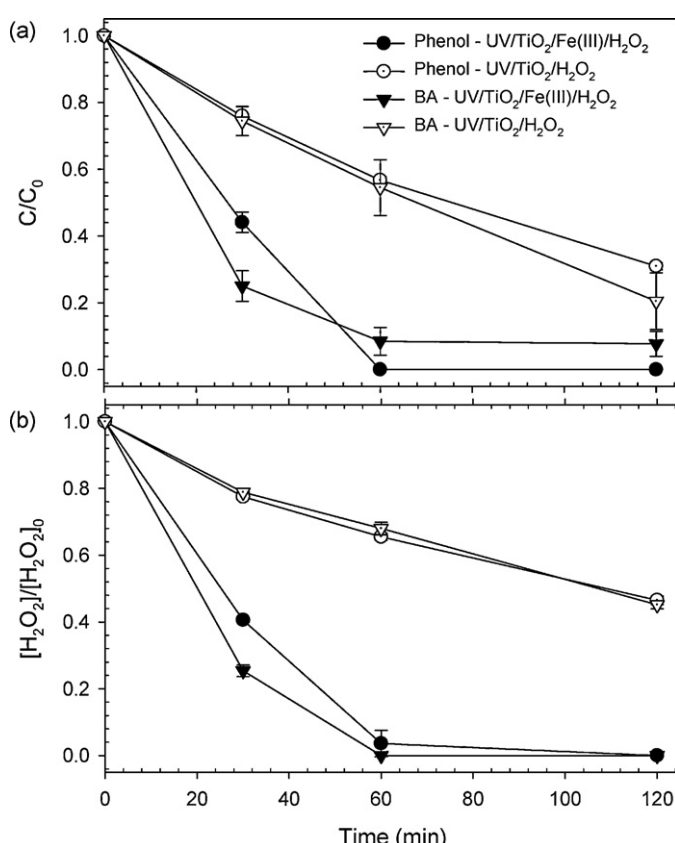
Fig. 3. Effect of Fe(III) on (a) degradation of phenol and benzoic acid and (b) decomposition of H_2O_2 ([Phenol]$_0$ = [Benzoic acid]$_0$ = 0.1 mM; [Fe(III)] = 0.25 mM; TiO_2 = 1 g/L; [H_2O_2] = 10 mM; pH_i 6).

H_2O_2 decay, which implies that the iron(III)-catalyzed decomposition of H_2O_2 likely enhances production of oxidizing species in the combined $UV/TiO_2/Fe(III)/H_2O_2$ system.

Fig. 4 provides a comparative analysis on the oxidation efficacies of phenol, benzoic acid, and methanol in five respective TiO_2 systems including, UV/TiO_2, $UV/TiO_2/H_2O_2$, $UV/TiO_2/Fe(III)$, $TiO_2/Fe(III)/H_2O_2$, and $UV/TiO_2/Fe(III)/H_2O_2$. Methanol oxidation was assessed by monitoring the formation of formaldehyde (HCHO), the primary oxidation product of methanol, in the presence of excess amount of methanol (200 mM). The $UV/TiO_2/Fe(III)/H_2O_2$ system exhibited the highest performance in terms of oxidation of all the three organic compounds, clearly showing the synergistic effects of the combination of TiO_2 photocatalysis and the Fenton-like system. For instance, the efficiency of the $UV/TiO_2/Fe(III)/H_2O_2$ system for organic oxidation exceeded the sums of the efficiencies of two individual systems such as, $UV/TiO_2/H_2O_2$ plus $UV/TiO_2/Fe(III)$, or $UV/TiO_2/H_2O_2$ plus $TiO_2/Fe(III)/H_2O_2$.

The addition of H_2O_2 to the UV/TiO_2 system resulted in greater oxidation of phenol and benzoic acid, which is likely attributed to the enhanced charge separation by H_2O_2 as an electron acceptor and the reductive conversion of H_2O_2 to $^\bullet OH$. Insignificant degradation of phenol and benzoic acid by the $TiO_2/Fe(III)/H_2O_2$ system confirmed the earlier findings that, the Fenton reaction does not effectively proceed under neutral pH conditions due to the H_2O_2 decomposition via a nonradical mechanism, which possible involves the formation of Fe(IV), which has a weaker oxidation power relative to $^\bullet OH$ [16,21]. The addition of Fe(III) to the UV/TiO_2 system negligibly affected the photocatalytic oxidation of phenol and even diminished the efficacy of the oxidation of benzoic acid (compare the UV/TiO_2 and $UV/TiO_2/Fe(III)$ systems), indicating that the ability of Fe(III) to serve as an electron acceptor and retard electron–hole recombination during the TiO_2 photocatalysis does not lead to kinetic enhancement in oxidation of organic compounds.
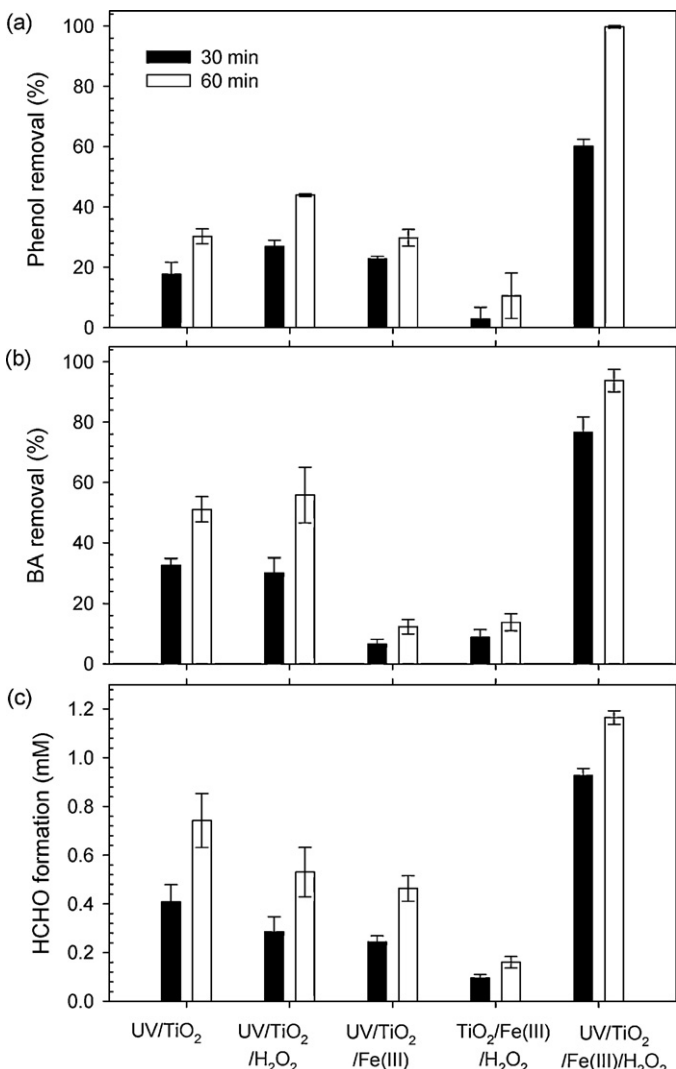
Fig. 4. Degradation of (a) phenol and (b) benzoic acid; and (c) formation of HCHO ([Phenol]$_0$ = [Benzoic acid]$_0$ = 0.1 mM; [Methanol]$_0$ = 200 mM; [Fe(III)] = 0.25 mM; TiO$_2$ = 1 g/L; [H$_2$O$_2$] = 10 mM; pH$_i$ 6).

The comparative analysis (Fig. 4a–c) shows that the oxidation efficacy is generally in the order of UV/TiO$_2$/Fe(III)/H$_2$O$_2$ > UV/TiO$_2$/H$_2$O$_2$ > UV/TiO$_2$ > UV/TiO$_2$/Fe(III) > TiO$_2$/Fe(III)/H$_2$O$_2$ regardless of the target organic compound, even if some substrate-specific behaviors (e.g., adsorption affinity) cause a slight deviation from the generalized trend. The presence of similar trends among methanol and aromatic compounds, such as phenol and benzoic acid imply that Fe(IV) is not involved in the oxidation of organic compounds to a significant extent in the combined UV/TiO$_2$/Fe(III)/H$_2$O$_2$ system. According to the recent studies [21–23], methanol is readily transformed into HCHO via oxidation by •OH as well as Fe(IV), whereas aromatic compounds are resistant to oxidation by Fe(IV). Therefore, if the formation of Fe(IV) is significant in the combined UV/TiO$_2$/Fe(III)/H$_2$O$_2$ system, the synergistic enhancement in oxidation should be more pronounced for methanol than benzoic acid or phenol.

3.3. Effects of Fe(III) concentration and pH

Fig. 5 demonstrates the influence of the concentration of Fe(III) added ([Fe(III)]$_0$) on the oxidative removal of phenol and benzoic acid in the UV/TiO$_2$/Fe(III)/H$_2$O$_2$ and the Fe(III)/H$_2$O$_2$ systems. A drastic increase in the removal efficiency with increasing [Fe(III)]$_0$
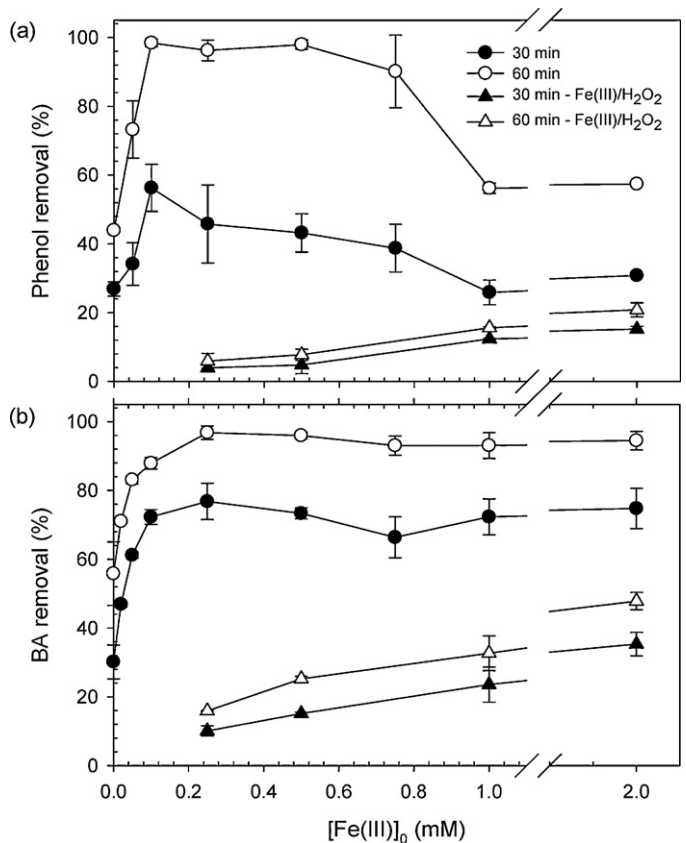
Fig. 5. Effect of Fe(III) concentration on degradation of (a) phenol and (b) benzoic acid (●,○: Fe(III)/TiO$_2$/H$_2$O$_2$/UV system and ▲,△: Fe(III)/H$_2$O$_2$ system) ([Phenol]$_0$ = [Benzoic acid]$_0$ = 0.1 mM; [Fe(III)] = 0.25 mM; TiO$_2$ = 1 g/L; [H$_2$O$_2$] = 10 mM; pH$_i$ 6).

was observed at the initial stage of [Fe(III)]$_0$ < 0.25 mM for both the cases of phenol and benzoic acid. There was a gradual decrease in the removal of phenol when [Fe(III)]$_0$ was further increased to 2 mM (Fig. 5a); whereas the removal efficiency of benzoic acid plateaued over the same range of [Fe(III)]$_0$ (Fig. 5b). The decrease in removal efficiency of phenol may result from UV-shielding by iron precipitates adsorbed on the surface of TiO$_2$ particles. The UV-shielding effect should also apply to the oxidation of benzoic acid, but the effect appears to be offset by the increasing contribution of the dark Fenton reaction with increasing [Fe(III)]$_0$. The phenol removal by the Fe(III)/H$_2$O$_2$ system was only 20% at 2 mM Fe(III) for 60 min reaction time (Fig. 5a), whereas the removal of benzoic acid reached over 46% under the identical conditions.

Fig. 6 demonstrates the efficiency of degradation of benzoic acid in six reaction systems including, Fe(III)/H$_2$O$_2$, UV/TiO$_2$, UV/TiO$_2$/H$_2$O$_2$, UV/TiO$_2$/Fe(III), TiO$_2$/Fe(III)/H$_2$O$_2$, and UV/TiO$_2$/Fe(III)/H$_2$O$_2$ as a function of pH. The Fenton-like reaction (the Fe(III)/H$_2$O$_2$ system) in the dark condition was effective only within the narrow pH range of 2–3, causing no significant degradation of benzoic acid under neutral and alkaline pH conditions. Notably, the dark Fenton-like reaction in the presence of TiO$_2$ particulates (the TiO$_2$/Fe(III)/H$_2$O$_2$ system) negligibly degraded benzoic acid even at acidic pH condition, which may be attributed to the limited availability of ferric ion for the homogeneous Fenton reaction, because of the facile adsorption of ferric ion on the TiO$_2$ surface. Almost constant removal efficiency of benzoic acid throughout the entire pH range in the UV/TiO$_2$ system confirmed the pH-independent photocatalytic activity of TiO$_2$. The addition of Fe(III) or H$_2$O$_2$ to the UV/TiO$_2$ system (compare the UV/TiO$_2$/H$_2$O$_2$ or UV/TiO$_2$/Fe(III) system to the UV/TiO$_2$ system) enhanced
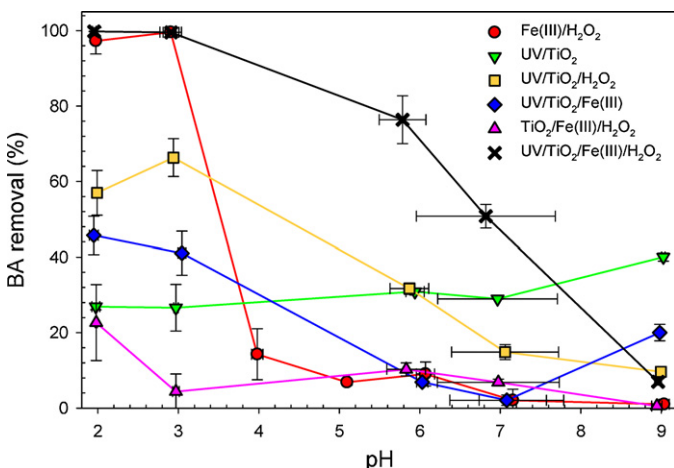
Fig. 6. Effect of pH on degradation of benzoic acid ([Benzoic acid]$_0$ = 0.1 mM; [Fe(III)] = 0.25 mM; TiO$_2$ = 1 g/L; [H$_2$O$_2$] = 10 mM; 10 mM borate buffer at pH 9; reaction time = 30 min; The horizontal error bars indicate the pH variation, the initial and final pHs.).

oxidation of benzoic acid at acidic pH, but conversely it caused the negative effects at higher pH values. As aforementioned, Fe(III) and H$_2$O$_2$ scavenges CB electrons to inhibit the electron–hole recombination in the photoexcited TiO$_2$. However, the change in speciation of Fe(III) and H$_2$O$_2$ with increasing pH (i.e., Fe(III)-oxyhydroxides or HO$_2$$^-$) lowers their electron-withdrawing activity, rendering Fe(III) and H$_2$O$_2$ function as electron donors to scavenge VB holes. In addition, the UV-shielding effect by iron precipitates is not negligible under neutral pH conditions. On the other hand, the combined UV/TiO$_2$/Fe(III)/H$_2$O$_2$ system clearly demonstrated the synergistic removal of benzoic acid at the pH values ranging from 4 to 7. The detailed mechanism of this synergism will be discussed in Section 3.5.

3.4. Effects of hole and •OH scavengers

Fig. 7 demonstrates the photocatalytic degradation of benzoic acid by UV/TiO$_2$/Fe(III)/H$_2$O$_2$ and the UV/TiO$_2$/H$_2$O$_2$ systems in the presence of scavengers of VB hole and •OH (i.e., formate and *tert*-butyl alcohol (t-BuOH)). Formate is capable of effectively scavenging both VB hole [24,25] and •OH (off and bound on TiO$_2$ surface) ($k_{•OH,formate}$ = 3.2 × 10^9 M^{-1} s^{-1}; [1]), while t-BuOH is primarily susceptible to oxidation by freely diffusing •OH in the bulk phase


Fig. 7. Scavenging efficiency of formate and *tert*-butyl alcohol ([Benzoic acid]$_0$ = 0.1 mM; [Fe(III)] = 0.25 mM; TiO$_2$ = 1 g/L; [H$_2$O$_2$] = 10 mM; pH$_i$ 6).

Scheme 1. Reaction pathways of oxidation of organic compounds in the UV/TiO$_2$/Fe(III)/H$_2$O$_2$ system.

($k_{•OH,t-BuOH}$ = 6.6 × 10^8 M^{-1} s^{-1}; [1]). The scavenging efficiency was calculated using the following equation.

$$\text{Scavenging efficiency} \ (\%) = \left(1 - \frac{k_s}{k}\right) \times 100 \qquad (1)$$
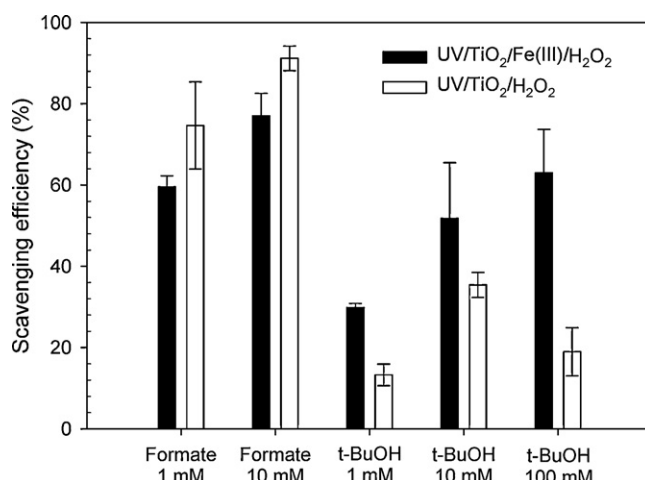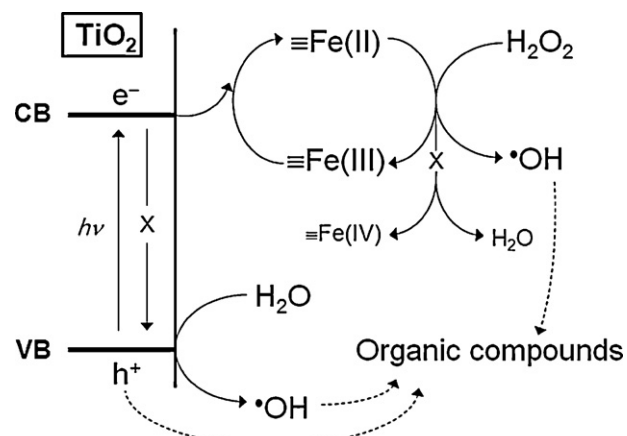
where k_s and k are the pseudo first-order rate constants for degradation of benzoic acid in the presence and absence of the scavengers, respectively.

A notable observation in Fig. 7 is that formate exhibited higher scavenging efficiency in the UV/TiO$_2$/H$_2$O$_2$ system when compared to the UV/TiO$_2$/Fe(III)/H$_2$O$_2$ system, whereas the influence of t-BuOH was more pronounced in the UV/TiO$_2$/Fe(III)/H$_2$O$_2$ system. This result indicates that the oxidation of benzoic acid by the UV/TiO$_2$/Fe(III)/H$_2$O$_2$ system relies more on the free •OH relative to the UV/TiO$_2$/H$_2$O$_2$ system, suggesting the possibility of additional route for the •OH production via the Fenton reaction in the UV/TiO$_2$/Fe(III)/H$_2$O$_2$ system.

3.5. Mechanism of enhanced oxidation of organic compounds in the UV/TiO$_2$/Fe(III)/H$_2$O$_2$ system

Dual roles of iron in the UV/TiO$_2$/Fe(III)/H$_2$O$_2$ system which offer reaction routes for synergistic production of •OH under neutral pH conditions are postulated in Scheme 1. First, Fe(III) adsorbed on the TiO$_2$ surface is reductively converted to ferrous ion (Fe(II)) via CB electron, with effective prevention of recombination of electron–hole pairs. The charge separation makes VB holes more available for oxidation of adsorbed organic compounds, and for oxidation of surface-bound hydroxyl groups and adsorbed water molecules into •OH. In particular, in combination with reoxidation of Fe(II) by H$_2$O$_2$ (confirmed by rapid H$_2$O$_2$ decay (Fig. 3b)), the reduction via CB electron enables the catalytic cycle of Fe(II)/Fe(III), thus maintaining a considerable concentration of Fe(III) as an electron acceptor. On the other hand, the systems in the absence of either photogenerated CB electron or H$_2$O$_2$ do not allow the effective reduction/reoxidation cycle, leading to accumulation of Fe(II) on TiO$_2$ surface and hindering electron-scavenging by iron. As a result, significant H$_2$O$_2$ decomposition (i.e. reoxidation of Fe(II)) did not occur in the TiO$_2$/Fe(III)/H$_2$O$_2$, the UV/Fe(III)/H$_2$O$_2$, and the Fe(III)/H$_2$O$_2$ systems (data not shown), and the UV/TiO$_2$/Fe(III) system did not lead to notable increase in the kinetics of oxidation of organic compounds (Figs. 4 and 6).

Second, the Fe(II) species bound to the photo-excited TiO$_2$ surface seemed to transform H$_2$O$_2$ into reactive oxidants capable of oxidizing phenol and benzoic acid at neutral pH (i.e., •OH). This assumption is inconsistent with the earlier findings that Fe(IV) and

its derivatives with selective reactivity rather than $^\bullet$OH are responsible for oxidation of organic compounds by the Fenton reaction occurring at neutral pH [2,21]. Moreover, heterogeneous iron catalysts exhibit extremely low efficiency in the oxidation of organic compounds at neutral pH due to the H_2O_2 decomposition via a non-radical mechanism [16,26], which may also be attributed to the formation of Fe(IV) on the catalyst surface and its rapid dissipation by the reaction with the adjacent Fe(II) [16,27]. However, as aforementioned, nonselective oxidation of target substrates including methanol, phenol, and benzoic acid in the UV/TiO$_2$/Fe(III)/H$_2$O$_2$ system (Figs. 4a–c) under neutral pH conditions was contradictory to the reported reactivity of Fe(IV) (i.e., Fe(IV) is known to oxidize methanol more selectively rather than aromatic compounds). In addition, the kinetic comparison in the presence of formate and t-BuOH as scavengers evidenced more critical contribution of $^\bullet$OH to oxidation of benzoic acid by the UV/TiO$_2$/Fe(III)/H$_2$O$_2$ system relative to the UV/TiO$_2$/H$_2$O$_2$ system (Fig. 7). Therefore, the results collectively suggest that the binding of iron to the photo-excited TiO$_2$ surface may affect the mechanism of the Fenton reaction to favor the production of $^\bullet$OH rather than Fe(IV) under neutral pH conditions. Similarly, it has been reported that soluble iron complexes with EDTA and POM [28,29] and iron oxide supported on the silica-alumina matrix [16] can enhance the oxidation pathway involving $^\bullet$OH during the Fenton reaction at neutral pH. The coordination of iron or iron oxide to ligands or supporting materials may modify the electronic properties of active Fe(II) species, thus switching the mechanism of the Fenton reaction between one electron (resulting $^\bullet$OH) and two electron (resulting Fe[IV]) transfers. Further research is needed for better understanding of the mechanisms through which the co-presence of Fenton-like reagent and photoactivated TiO$_2$ surface influence the Fenton reaction at neutral pH and in identifying the reactive oxidant responsible for the oxidation of organic compounds in the combined system (i.e., whether it is $^\bullet$OH or other forms of Fe(IV); [28,30–32]).

4. Conclusions

This study demonstrated that the combination of TiO$_2$ photocatalysis and the Fenton-like reaction (i.e., the UV/TiO$_2$/Fe(III)/H$_2$O$_2$ system) synergistically accelerated oxidative degradation of organic compounds at circumneutral pH. Kinetic experiments on the oxidation of phenol, benzoic acid, and methanol under various combined systems clearly showed the synergistic increase of the reactive oxidant in the UV/TiO$_2$/Fe(III)/H$_2$O$_2$ system over pH 4–7. The observed synergism is attributed to (i) the electron-scavenging effect of Fe(III) adsorbed on the TiO$_2$ surface and (ii) the additional production of reactive oxidant by the Fenton reaction. Notably, the Fenton reaction, which occurred on the photoexcited TiO$_2$ surface appeared to produce a more reactive oxidant (e.g., $^\bullet$OH) than the Fe(IV) species, which was usually formed by the Fenton reaction at neutral pH. As a result, the integrated UV/TiO$_2$/Fe(III)/H$_2$O$_2$ system can enhance the rate of contaminant oxidation by increased production of reactive oxidants as well as broaden the range of degradable contaminants by further improvement in the reactivity of the oxidant produced from the Fenton reaction.

Acknowledgments

References

[1] G.V. Buxton, C.L. Greenstock, W.P. Helman, A.B. Ross, J. Phys. Chem. Ref. Data 17 (1988) 513–886.
[2] C. Lee, D.L. Sedlak, J. Mol. Catal. A: Chem. 311 (2009) 1–6.
[3] G.P. Anipsitakis, D.D. Dionysiou, Environ. Sci. Technol. 37 (2003) 4790–4797.
[4] B. Yue, Y. Zhou, J.Y. Xu, Z.Z. Wu, X.A. Zhang, Y.F. Zou, S.L. Jin, Environ. Sci. Technol. 36 (2002) 1325–1329.
[5] J.G. Lin, Y.S. Ma, J. Environ. Eng.: ASCE 126 (2000) 130–137.
[6] J.J. Pignatello, E. Oliveros, A. MacKay, Crit. Rev. Environ. Sci. Technol. 36 (2006) 1–84.
[7] N. Remya, J.G. Lin, Chem. Eng. J. 166 (2011) 797–813.
[8] M.R. Hoffmann, S.T. Martin, W.Y. Choi, D.W. Bahnemann, Chem. Rev. 95 (1995) 69–96.
[9] J.S. Lee, W.Y. Choi, J. Phys. Chem. B 109 (2005) 7399–7406.
[10] K. Tanaka, K. Abe, C.Y. Sheng, T. Hisanaga, Environ. Sci. Technol. 26 (1992) 2534–2536.
[11] W.G. Barb, J.H. Baxendale, P. George, K.R. Hargrave, Trans. Faraday Soc. 47 (1951) 591–616.
[12] C. Flox, S. Ammar, C. Arias, E. Brillas, A.V. Vargas-Zavala, R. Abdelhedi, Appl. Catal. B: Environ. 67 (2006) 93–104.
[13] W.Y. Choi, A. Termin, M.R. Hoffmann, J. Phys. Chem. 98 (1994) 13669–13679.
[14] J. Arana, O.G. Diaz, J.M.D. Rodriguez, J.A.H. Melian, C.G.I. Cabo, J.P. Pena, M.C. Hidalgo, J.A. Navio-Santos, J. Mol. Catal. A: Chem. 197 (2003) 157–171.
[15] M. Asilturk, F. Sayilkan, E. Arpac, J. Photochem. Photobiol. A 203 (2009) 64–71.
[16] A.L.T. Pham, C. Lee, F.M. Doyle, D.L. Sedlak, Environ. Sci. Technol. 43 (2009) 8930–8935.
[17] C.G. Hatchard, C.A. Parker, Proc. R. Soc. Lond. Ser. A 235 (1956) 518–536.
[18] X.L. Zhou, K. Mopper, Mar. Chem. 30 (1990) 71–88.
[19] G. Eisenberg, Ind. Eng. Chem. Anal. Ed. 15 (1943) 327–328.
[20] H. Tamura, K. Goto, YotsuyanT., M. Nagayama, Talanta 21 (1974) 314–318.
[21] C.R. Keenan, D.L. Sedlak, Environ. Sci. Technol. 42 (2008) 1262–1267.
[22] S.J. Hug, L. Canonica, M. Wegelin, D. Gechter, U. Von Gunten, Environ. Sci. Technol. 35 (2001) 2114–2121.
[23] S.J. Hug, O. Leupin, Environ. Sci. Technol. 37 (2003) 2734–2742.
[24] V.N.H. Nguyen, R. Amal, D. Beydoun, Chem. Eng. Sci. 58 (2003) 4429–4439.
[25] T. Tan, D. Beydoun, R. Amal, J. Photochem. Photobiol. A 159 (2003) 273–280.
[26] Y.N. Lee, R.M. Lago, J.L.G. Fierro, J. Gonzalez, Appl. Catal. A: Gen. 215 (2001) 245–256.
[27] R. Gonzalez-Olmos, F. Holzer, F.D. Kopinke, A. Georgi, Appl. Catal. A: Gen. 398 (2011) 44–53.
[28] C. Lee, C.R. Keenan, D.L. Sedlak, Environ. Sci. Technol. 42 (2008) 4921–4926.
[29] C.R. Keenan, D.L. Sedlak, Environ. Sci. Technol. 42 (2008) 6936–6941.
[30] J. Jiang, S.Y. Pang, J. Ma, Environ. Sci. Technol. 42 (2008) 8167–8168.
[31] C.H. Lee, C.R. Keenan, D.L. Sedlak, Environ. Sci. Technol. 42 (2008) 8169.
[32] C.K. Remucal, C. Lee, D.L. Sedlak, Environ. Sci. Technol. 45 (2011) 3177–3178.